Invariant curves of analytic perturbed nontwist area preserving maps

Carles Simó

Departament de Matemàtica Aplicada i Anàlisi
Universitat de Barcelona
Gran Via 585, 08007 Barcelona (Spain)

Abstract

Area preserving maps close to integrable but not satisfying the twist condition are studied. The existence of invariant curves is proved, but they are no longer graphs with respect to the angular variable. Beyond the generic, codimension 1 case, several higher codimension cases are studied. Meandering curves, higher order meandering and labyrinthic curves show up. Several examples illustrate that this behavior occurs in very simple families of maps.

1 Introduction

It is well known that Hamiltonian systems with two degrees of freedom give rise, by means of a Poincaré section on a fixed level of energy, to area preserving maps (APM) (see, e.g., [12] §22). This supplies a powerful tool to understand the dynamics and to obtain stability criteria. To this end one requires the map to be (at least locally) a small enough perturbation of a twist map. To be more concrete, assume the map is expressed in polar coordinates (x the angle mod 2π, y the radius) as

$$(x, y) \to (x + \alpha(y), y) + \varepsilon(f_1(x, y), f_2(x, y)), \qquad (1)$$

where y ranges on some interval, $[y_1, y_2]$, $0 < y_1 < y_2$ and $x \in \mathbb{S}^1$. The terms f_1, f_2 appearing in the *perturbation* are not independent, the full map having to satisfy the APM condition. The first (*unperturbed*) part of the map in (1) has a dynamics foliated by invariant circles and is said to satisfy a *twist condition* if $|d\alpha/dy|$ is bounded from below in $[y_1, y_2]$. Then, if ε is small enough, some invariant curves subsist under the perturbation. If for some $y^* \in (y_1, y_2)$ one has that $\rho = \alpha(y^*)/(2\pi)$ satisfies a diophantine condition, $|\rho - p/q| > c/q^\tau$ for any $p/q \in \mathbb{Q}$, $(p, q) = 1$, $q > 0$ and some positive c and τ, then an invariant curve exists with rotation number ρ if ε is small enough. Furthermore, it can be expressed as the graph of a function, $y = g(x)$, defined on $\mathbb{S}^1$.

This is the contents of the celebrated *Moser twist theorem*. The analytic case belongs to the so called KAM theory [7, 1], the first proof in the differentiable case being done by Moser [8] and successive improvements, concerning optimality of the differentiability condition, being mainly due to Rüssmann [11] and Herman [5]. We shall not pursue in this direction. Our main concern will be to clarify the situation when the twist condition is no longer satisfied. Some results in this direction and a lot of inspiring ideas can be found in Herman [6]. To simplify things we shall keep our study in the analytic context, but this is not essential for any of the results.

The main idea is that one can recover easily a twist condition if a suitable change of variables is done, to *adapt coordinates to the dynamics*. In particular one has to choose a convenient scaling of the variables. We shall start with an integrable case where the twist condition is no longer satisfied with the lower codimension: there is some value of y^* such that $d\alpha/dy(y^*) = 0$, but $d^2\alpha/dy^2(y^*) \neq 0$. Generic perturbations and the corresponding unfolding of this situation display invariant curves which, of course, are no longer graphs over $\mathbb{S}^1$. Several "natural" examples are displayed. Furthermore, just to illustrate that the examples are not degenerated at all, one of the very "popular" families of maps is considered. The conservative Hénon map is enough to display the occurrence of the phenomenon studied here. The invariant curves which show up have a kind of "meandering" behavior (like the path of an old river on a flat country). *Higher order meandering* can occur, again in very simple families of maps, if the suitable parameter ranges are selected.

Then we turn to nongeneric perturbations, which can give rise to invariant curves with different patterns. Also the nongeneric case, concerning the degeneracy of the twist, is considered. Some results in case the first nonzero derivative of $\alpha(r)$ at $y = y^*$ is of order k, $k > 2$, are given.

If nongeneric conditions on the twist are combined with nongeneric perturbations, higly degenerate and interesting examples can be shown, giving rise to what can be name as *labyrinthic* invariant curves. Again they show up in very simple examples.

At this point it is interesting to remark that all the cases considered are robust in front of small perturbations. This follows from the robustness of the diophantine invariant curves of (1) when f_1 and f_2 have a sufficiently small perturbation. In particular, for all the families of maps used in the examples (even the nongeneric ones), meandering curves exist for open sets of the space of parameters.

For shortness all the examples given here use simple discrete maps. Certainly the phenomena displayed occur on Poincaré sections in mechanical problems.

We close with an outlook to related cases and further problems.

2 Perturbation of one–parameter families of nontwist maps. The generic case

Without loss of generality we can assume that the critical value, y^*, of y is located at the origin. Our initial integrable case, F_0, can be put in the form

$$F_0 : (x, y) \to (\bar{x}, \bar{y}) = (x + \omega + y^2 + O(y^3), y), \tag{2}$$

where $\alpha(y)$ is assumed to be analytical in a neighborhood of $y = 0$ and the y variable has been scaled to get the coefficient 1 in front of the y^2 term. Note that, according to (2), F_0 has a minimum of the rotation number at $y = 0$. In a similar way we can study the case of a maximum.

It is convenient to work with the generating function, S, of an APM, F, instead of working with $F:(x,y)\to(\bar{x},\bar{y})$ itself:

$$S=S(x,\bar{y}),\quad \bar{x}=\frac{\partial S}{\partial \bar{y}},\quad y=\frac{\partial S}{\partial x}.$$

So, the generating function, S_0, corresponding to (2) is given by

$$S_0(x,\bar{y})=x\bar{y}+\omega\bar{y}+\frac{1}{3}\bar{y}^3+O(\bar{y}^4). \tag{3}$$

Now we proceed to perturb (2) from F_0 to some ε–depending family, F_ε. As already said, it is simpler to perturb the generating function to S_ε. The main result is as follows.

Theorem 1 (Generically perturbing the generic case)
Consider a generic perturbation of a nontwist APM given by the generating function in (3). Then it has invariant curves, if the perturbation is small enough, for ω in suitable ranges.

Proof The proof consists of several steps.

Step 1: Reduction to a model plus small perturbations

Let us consider the generating function of the perturbed map. It is of the form

$$S_\varepsilon(x,\bar{y})=x\bar{y}+\omega\bar{y}+\frac{1}{3}\bar{y}^3+O(\bar{y}^4)+\Sigma_{j\geq 1}\varepsilon^j\Sigma_{k\geq 0}p_{j,k}(x)\bar{y}^k, \tag{4}$$

where ε is a small parameter and $p_{j,k}$ are 2π–periodic functions, so that S_ε is analytic on some domain $|\bar{y}|<y_0$, $|\mathrm{Im}(x)|<x_0$. From (4) it follows that the dominant terms of the perturbed map, F_ε, are

$$\bar{x}=x+\omega+\bar{y}^2+O(y^3,\varepsilon),\quad \bar{y}=y-\varepsilon\frac{dp_{1,0}}{dx}+O(\varepsilon y,\varepsilon^2). \tag{5}$$

We shall assume (and this is generic) that $\dfrac{dp_{1,0}}{dx}$ is not identically zero, and, for shortness, it will be denoted simply as $-p(x)$, a 2π–periodic function with zero average. The form of (5) suggest the scalings

$$y\to\gamma y,\quad \gamma=\varepsilon^{1/3},\quad \omega=2\pi\frac{m}{n}+\delta,\quad \delta=-b\alpha,\quad \alpha=\varepsilon^{2/3}, \tag{6}$$

where b and the new variable y (that we shall denote again as y) are assumed to be finite in the zone of interest. Hence, we are looking at a strip of width $O(|\varepsilon|^{1/3})$ in the original y variable and the parameter ω of the original map is considered on an $O(|\varepsilon|^{2/3})$–neighborhood of a suitable rational, m/n. From now on it is more convenient to look at α as the current small parameter.

Hence, the new format of the map, after the scalings in (6), is

$$F_\alpha:\ (x,y)\to(\bar{x},\bar{y})=\left(x+2\pi\frac{m}{n}+\alpha(-b+\bar{y}^2)+O(\alpha^{3/2}),y+\alpha p(x)+O(\alpha^{3/2})\right). \tag{7}$$

Assuming α very small compared to $1/n$, it is natural to look for the n–th power of F_α, the terms independent of α being reduced to the identity. Let $(x^{(0)}, y^{(0)})$ be an initial point and $\{(x^{(j)}, y^{(j)}),\ j = 1,\ldots,n\}$ the n first iterates under (7). A simple computation gives

$$F_\alpha{}^n : \begin{pmatrix} x^{(0)} \\ y^{(0)} \end{pmatrix} \to \begin{pmatrix} x^{(n)} \\ y^{(n)} \end{pmatrix} = \begin{pmatrix} x^{(0)} + n\alpha(-b + (\bar{y}^{(0)})^2) + O(n\alpha^{3/2}) \\ y^{(0)} + \alpha\Sigma_{j=0}^{n-1} p(x^{(j)}) + O(n\alpha^{3/2}) \end{pmatrix}. \tag{8}$$

The summation in (8) can be expressed as

$$n\{c_n \sin(nx^{(0)} + \varphi_n) + c_{2n}\sin(2nx^{(0)} + \varphi_{2n}) + \ldots\} + O(n\alpha^2), \tag{9}$$

where φ_{kn}, $k \geq 1$, are suitable phases. Again the genericity allows to assume that $c_n \neq 0$ and, to simplify the discussion in what follows, we make use of the analyticity of p to assume also that the coefficients c_{kn} are much smaller than c_n, for $k \geq 2$, so that we only keep c_n in what follows, the neglected terms producing only small deformations. Anyway, cases where this assumption does not hold will be considered later.

Now we are in situation to do the following reductions:

1) As the relevant angle in (9) is $nx^{(0)}$ we shall consider it as new angular variable. Again, it will be denoted simply as x. In a similar way, $y^{(0)}$ will be denoted as y.

2) The phase φ_n can be skipped by means of a shift of the origin of angles.

3) The parameter $n\alpha$ can be considered to be the new small parameter. We shall denote it again as α.

4) The coefficient c_n can be scaled to 1, by a suitable scaling of the y variable (and the subsequent rescaling of α). This implies also a scaling of b, but we shall keep the same name for the new parameter.

Summarizing, the map in (8) can we written, essentially, as the model map

$$M_\alpha : (x, y) \to (\bar{x}, \bar{y}) = \Big(x + \alpha(-b + \bar{y}^2) + o(\alpha), y + \alpha\sin(x) + o(\alpha)\Big). \tag{10}$$

It is still an APM and, because of the smallness of α, it is close to the identity. The usual methods of suspension to a one degree of freedom time–periodic Hamiltonian flow and averaging (see [9] for the general framework and [2] for one more adapted to the present setup) assure that the map M_α in (10) can be written as the time α flow of an autonomous Hamiltonian plus an exponentially small error in α (i.e., bounded by an expression of the form $\exp(-c_1/|\alpha|)$ for some positive c_1 and α small enough). Furthermore, the Hamiltonian has the form

$$H_\alpha(x, y) = -by + \frac{1}{3}y^3 + \cos(x) + o(1), \tag{11}$$

when α goes to 0, the dependence on α being included in the $o(1)$ term, on a compact domain in the (x, y, b) variables, including, for instance, $\mathbb{S}^1 \times [-10, 10] \times [-10, 10]$. This is enough for our purposes.

Step 2: Study of the Hamiltonian

Now we should study the dynamics of (11), skipping the $o(1)$ terms, as a function of b. Fixed points appear for $b \geq 0$. They are located at $A = (0, \sqrt{b})$, $B = (0, -\sqrt{b})$, $C = (\pi, \sqrt{b})$ and $D = (\pi, -\sqrt{b})$. If $b > 0$, A and D are hyperbolic, the other two being elliptic. If $b = 0$ then $A = B$, $C = D$ and both are parabolic. It is interesting to note that the values of the Hamiltonian at the different fixed points are

$$H(A) = -\frac{2}{3}b^{3/2}+1, \quad H(B) = \frac{2}{3}b^{3/2}+1, \quad H(C) = -\frac{2}{3}b^{3/2}-1, \quad H(D) = \frac{2}{3}b^{3/2}-1. \quad (12)$$

From (12) it follows that for the critical value $b_{crit} = (3/2)^{2/3}$ the hyperbolic points are on the same level of energy ($H = 0$). Hence, beyond homoclinic connections there will be heteroclinic ones for this value of b.

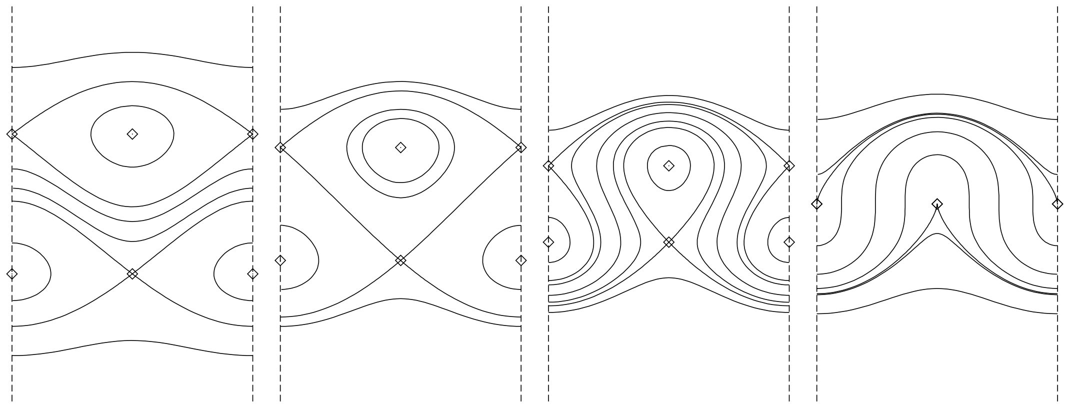

Figure 1: Several scenarios for the behavior of the Hamiltonian flow given by (11).

Figure 1 shows an illustration of the phase portrait of (11) for different values of b. Plots a) to d) go from left to right. In figure 1 a) the case $b > b_{crit}$ is shown. Points with large values of $|y|$ move to the right, while for $|y|$ small they move to the left: the two resonant zones are separated. The case b) corresponds to the critical one, when the heteroclinic connection occurs: the resonances start to merge. Case c), with $b \in (0, b_{crit})$, is the most interesting for our purposes: the resonances interfere. The points on the range of energies $h \in (\frac{2}{3}b^{3/2} - 1, 1 - \frac{2}{3}b^{3/2})$ move now on orbits which flow, on the average, from left to right, but they move to the left between the y levels of the fixed points. We shall denote the integral curves on this range as *meandering curves*. Finally, figure 1 d) displays the case $b = 0$, all nonfixed points moving monotonically to the right. For $b < 0$ no fixed points appear and all points move to the right: the resonances are gone.

Now we concentrate on the case shown in figure 1 c). The meandering curves are periodic orbits whose period depends only on b and $|h|$ because of symmetry reasons. It is clear that, for a fixed b, the period increases to ∞ when $|h|$ increases to $H(A)$. It would be nice (but not essential for our purposes) to have a monotonic behavior of the period with respect to $|h|$. This seems to be the case, based on exhaustive numerical checks, but, for the moment being, we can only formulate it as

Conjecture 2 *For $b \in (0, b_{crit})$ the period of the meandering curves is an increasing function of $|h|$.*

If we consider the period $T(b,|h|)$ for $h=0$, the following holds

Lemma 3 *The period of the meandering curves of (11), in the limit when α goes to zero, for the energy level $h=0$, $T(b,0)$, is an increasing function of b in the range $(0,b_{crit})$.*

Proof (of the Lemma) In this case the period is given by

$$T(b,0)=4\int_0^{y_{max}}\left(1-(by-y^3/3)^2\right)^{-1/2}dy, \tag{13}$$

where y_{max} is the unique real zero of $by=y^3/3-1$. It is obvious that y_{max} is an increasing function of b, and it ranges in $(3^{1/3},12^{1/3})$. Hence, as introducing $z=y/y_{max}$ the period is expressed as

$$T(b,0)=4y_{max}\int_0^1\left(1-(y_{max}^3(z-z^3)/3-z)^2\right)^{-1/2}dz, \tag{14}$$

it is enough to check that $T(b,0)$ increases with y_{max}. Introducing $\gamma=y_{max}^3/3$, which ranges in $(1,4)$ and $w=z^2$, the next expression follows from (14)

$$\frac{dT(b,0)}{dy_{max}}=2\int_0^1 A(\gamma,w)B(\gamma,w)^{-3/2}w^{-1/2}(1-w)^{-1/2}dw, \tag{15}$$

where

$$A(\gamma,w)=1+w(2\gamma^2-\gamma)-w^2 2\gamma^2,\quad B(\gamma,w)=1+w(2\gamma-\gamma^2)+w^2\gamma^2.$$

The following properties of the functions A and B are easy to check:

- $A(\gamma,\cdot)$ has an unique zero, $w_c(\gamma)$, in$(0,1)$, for all $\gamma\in(1,4)$. Furthermore $w_c(\gamma)\geq 8/9$, the equality being achieved for $\gamma=9/4$. The function A has an unique maximum in $[0,w_c]$.
- $A(\gamma,w)\geq 1$ if $w\in[0,1/2]$, $\forall\gamma\in[1,4]$. Also $A(\gamma,w)\geq -3$, $\forall w\in[0,1]$, $\forall\gamma\in[1,4]$.
- $B(\gamma,\cdot)$ is increasing if $\gamma\leq 2$, and has an unique minimum located at $1/2-1/\gamma$ if $\gamma\in(2,4]$, where it takes the value $\gamma-\gamma^2/4$.
- $B(\gamma,w)\leq 2$, $\forall w\in[0,1/2]$, $\forall\gamma\in[1,4]$. On the other side, $B(\gamma,w)\geq 217/81>8/3$, $\forall w\in[8/9,1]$, $\forall\gamma\in[1,4]$.

Then, as in (15) we can write $\int_0^1=\int_0^{1/2}+\int_{1/2}^{w_c}+\int_{w_c}^1$, and the inequalities

$$\int_0^{1/2}>2^{-3/2}\int_0^{1/2}w^{-1/2}(1-w)^{-1/2}dw,\ \int_{1/2}^{w_c}>0,\ |\int_{w_c}^1|<3(8/3)^{-3/2}\int_0^{1/9}w^{-1/2}(1-w)^{-1/2}dw$$

hold, it is enough to check

$$8\int_0^{1/2}w^{-1/2}(1-w)^{-1/2}dw>3^{5/2}\int_0^{1/9}w^{-1/2}(1-w)^{-1/2}dw,$$

which is obviously true. $\square$

Note that for $b=0$ one reaches the minimum value of $T(b,0)$:

$$T(0,0)=4\times 3^{1/3}\Sigma_{j\geq 0}\frac{(2j-1)!!}{(2j)!!}\frac{1}{6j+1}\simeq 7.005440706685.$$

Therefore, the rotation number of the time α flow of the limit Hamiltonian (11), for the orbit in a level of energy h and a given value of the parameter b, is $\rho(\alpha,b,h)=\alpha/T(b,|h|)$. This rotation number has a nonzero derivative, except at $h=0$ and, eventually, at some other value of h. (In fact there are no other exceptional values if the Conjecture above is true).

Step 3: Back to the diffeomorphism and existence of invariant curves

Now we go back to the diffeomorphism M_α defined in (10). But first, for a given value of $b\in(0,b_{crit})$, we know that it is possible to pass to *action–angle* variables for $h\in(H(D),H(A))$. Let (I,ψ) be these variables, where I can be taken to be h and ψ as the scaled arc length. The change of variables is a nice diffeomorphism (that is, with bounded differential and inverse of the differential) except for values of $|h|$ too close to $1-\frac{2}{3}b^{3/2}$. For a detailed account about how to proceed to bound the effect of the change of variables, see [2], where the computations are done in the study of Bogdanov–Takens diffeomorphisms. In the (I,ψ) variables the time α flow of H_α is written as

$$(I,\psi)\rightarrow(I,\psi+2\pi\rho(\alpha,b,h)) \tag{16}$$

Note that in H_α we should consider not only the "dominant" term, but the full expression, so that the difference between the time α flow and M_α is exponentially small in α. Now we are ready to write M_α in the (I,ψ) variables:

$$M_\alpha:(I,\psi)\rightarrow(\bar{I},\bar{\psi})=(I,\psi+2\pi\rho(\alpha,b,h))+O(\exp(-c_2/\alpha)), \tag{17}$$

where the new constant, c_2, is still positive, but is has decreased with respect to the previous constant, c_1, to take into account the deformations introduced by the change of variables.

The map (17) is now a relatively small perturbation of a twist map. Despite the twist is "small" (it is of the order of α and, furthermore, contains a factor going to zero when the related $|h|$ goes to $1-2b^{3/2}/3$), the perturbation is so small that one can still apply the original Moser's theorem to prove the existence of invariant curves, close to the ones of H_α, that is, with the *meandering character.*

These curves can not approach too closely the homoclinic connections of the limit flow (see figure 1 case c)) because of the generic splitting of separatrices and the associated *stochastic zone*, but this affects, in any case, an exponentially narrow strip.

□

3 Examples. Higher order meandering curves

We start with simple examples to illustrate Theorem 1. For the first example (see figure 2 a)) we use the family of maps

$$F_{\omega,\alpha,\beta}:(x,y)\rightarrow\left(\bar{x}=x+2\pi\omega+\bar{y}^2,\bar{y}=y+\alpha\frac{\sin(x)}{1-\beta\cos(x)}\right). \tag{18}$$

This family of maps still has some symmetry properties, due to the odd character of the terms appearing in (18) inside $\bar{y}$, but is not so degenerate as the case with $\beta = 0$, as we shall see later. The effect of β is to produce infinitely many harmonics. For figure 2 *a*) the values used are: $\omega = 0.249$, $\alpha = 0.1$, $\beta = 0.5$, so m/n is $1/4$. Eight islands are easily seen. They belong to two families of 4–periodic islands and, between these families, the meandering curves appear. As predicted by the theoretical analysis in §2, the elliptic points at the center of the two families of islands have x values which are roughly shifted by π/n. For figure 2 *b*) we used the same map with parameters $\omega = 0.374675$, $\alpha = 0.1$, $\beta = 0.5$, so m/n is $3/8$ and the corresponding two families of 8–periodic islands and meandering curves can also be seen.

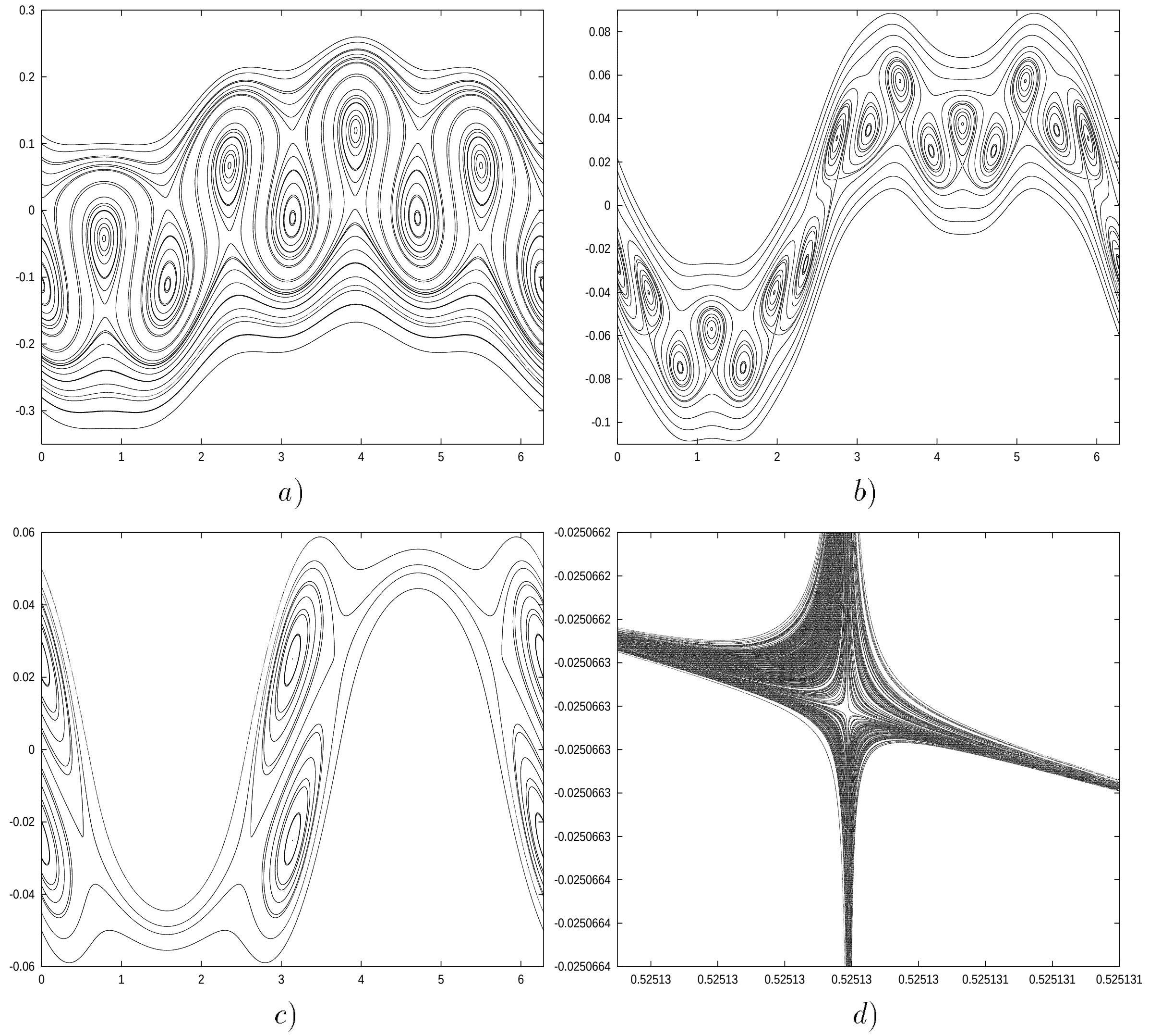

Figure 2: Several examples of meandering curves. *a*) and *b*) are generic cases. *c*) is a nongeneric case, and *d*) is a magnification of *c*). In all the plots, except *d*), the horizontal window is $[0, 2\pi]$. Vertical windows: $[-0.35, 0.3]$ in *a*), $[-0.11, 0.09]$ in *b*), $[-0.06, 0.06]$ in *c*). In *d*) the window $[0.5251295, 0.525131] \times [-0.0250664, -0.0250662]$ has been used. See the text for the maps and parameters used.

On the other side, in figure 2 *c*) the parameters are $\omega = 0.4999$, $\alpha = 0.1$, $\beta = 0$, so m/n is $1/2$. As $\beta = 0$ this map can be seen as a (loosely speaking) *nontwist standard* *map*. It is degenerate in the sense that it contains just one harmonic. Doing n iterates it averages "too well" and it is nongeneric. Now there are still two families of 2–periodic islands, but the elliptic points at the centers of the islands are, roughly, at the same x values for both families. No meandering curves are seen, but in §4 we shall study this situation. A particular case of this map, having $\omega = 0$, is named *quadratic standard map*. This case as well as the *trigonometric standard map* (where the $\bar{x} = x + \bar{y}$ part of the standard map is replaced by $\bar{x} = x + \alpha \sin(\bar{y})$), are exemplified in [4], where additional meandering curves can be seen. The trigonometric standard map is also known as "the" *twist map*, as introduced in [15]. Some properties and generalizations can be found in [10] and in [3], Appendix C.

The three pictures presented here look as "quite integrable". To make evident that they are nonintegrable we can take initial conditions close to one of the points in one of the two hyperbolic orbits. We did this for the case in *c*) and a magnification (in a very small window) is displayed in figure 2 *d*). All the points shown belong to the same orbit (5 million iterates have been computed but only a few fall in the window). The size of the "chaotic sea" near the saddle is of the order 10^{-7} and, so, we can expect that the splitting of the separatrices which creates this chaotic region is of the order of 10^{-14}. This should go very quickly to zero when decreasing α, due to the exponentially small character of the *nonintegrable remainder*.

A very natural question is whether the meandering curves appear in simple and very "popular" APM or, despite the genericity, we have to look for them is some "strange enough" families. The answer to this question is that, in some sense, they should appear in "all" families of maps. It is well known that, in an elliptic island, the analytic APM tend to behave (locally) like the Hénon map, at a small scale. Hence, we have checked that case (see also [13, 14] where meandering curves are seen inside period 3 islands of the separatrix map, another "universal" model).

For reference, the version of the Hénon map we use is

$$HM_\varepsilon : (x, y) \to (\bar{x}, \bar{y}) = (x + \bar{y}, y - x(x - \varepsilon)). \tag{19}$$

According to (19), HM_ε has fixed points at $(0, 0)$ (hyperbolic if $\varepsilon > 0$) and at $(\varepsilon, 0)$ (elliptic if $\varepsilon \in (0, 4)$). Around the elliptic fixed point, except in the case $\varepsilon = 3$, for which the eigenvalues at that point are cubic roots of the unity, there are invariant islands around the fixed point. It is possible to compute the rotation number of the invariant curves. Of course, for some initial values we shall not be on an island but on a chaotic zone and, in that case, the average rotation of the map will have a wild behavior.

Figure 3 shows the rotation number $\rho(x_{in}, \varepsilon)$ as a function of x_{in}, starting the iterations at $(x_{in}, 0)$. For a given value of ε the different values of ρ are joined, arbitrarily, by a line. For ε between, roughly, 2.5 and 2.83, the rotation number passes through a maximum before the curves are destroyed. For rationals inside the range $(0.28, 0.33)$ (roughly), meandering curves appear. An example for ρ near $4/13$ is displayed in figure 3. For (19) a normal form computation around the elliptic point shows that the first Birkhoff coefficient changes sign (from negative to positive) between $\varepsilon = 2$ and $\varepsilon = 3$.

A very interesting question appears when we consider "the iteration of the process". That is, in the "central domain" of meandering curves of M_α (see (10)), which in the Hamiltonian approximation corresponds to the level $H_\alpha = 0$ (see (11) and figure 1) the

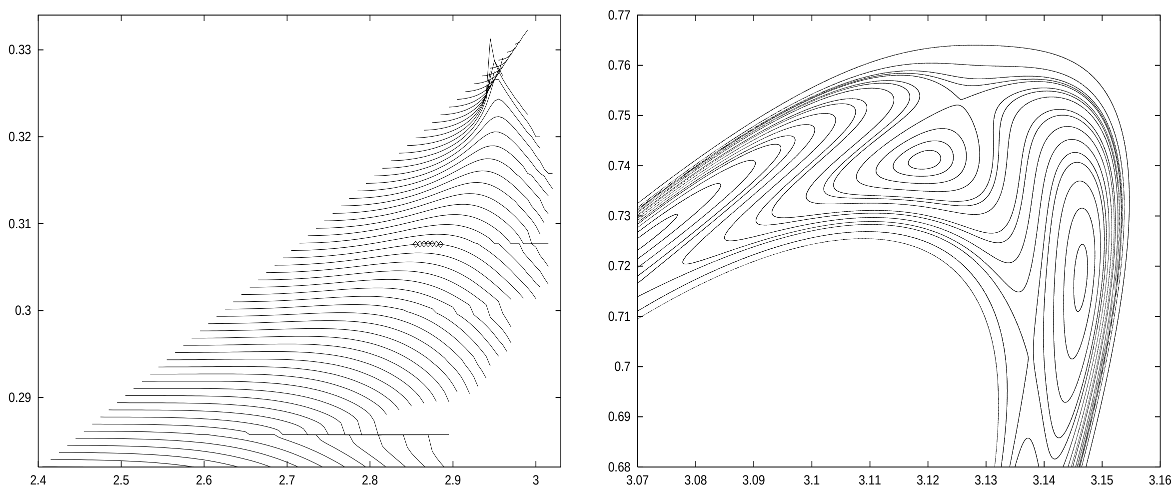

Figure 3: Left: The rotation number, ρ, as a function of the initial x coordinate (with $y = 0$) for the Hénon map, as given by (19). Different lines correspond to different values of ε. The horizontal axis shows the values of x_{in}, while the vertical one shows the values of ρ. The zone displayed here corresponds to values of the rotation number between 1/4 and 1/3. The points marked on the figure indicate the values where a maximum of ρ, close to 4/13, is obtained. Right: Magnification of the results of a simulation using the value $\varepsilon = 2.68998$, for which meandering curves can be seen, as well as two islands with rotation number 4/13.

rotation number has a maximum, and, by a suitable choice of the parameter α one can obtain that this rotation number is close enough to a rational. Then we shall be in situation to apply Theorem 1 again, and the process can be iterated as many times as desired. We refer to figure 4, to be commented later.

If we start with a meandering curve, we can call it a *first order meander*. Then, we can look at this curve in the action–angle variables introduced in Step 3 of the proof of Theorem 1. It will be quite close to a circle, with no meandering at all. Close to the central part, for a suitable rotation number, a meander can appear in these coordinates. It will be denoted as *second order meander*. In a similar way *higher order meanders* are introduced.

Figure 4 shows an illustration of this situation. Subfigures *b*), *c*) and *d*) are successive magnifications of *a*). In all of them a third order meander is shown. Furthermore, in *d*) there are other invariant curves, two of them being fourth order meanders (three more are invariant curves in periodic islands). Notice that we start here the plots with third order meanders. In fact, for the values of the parameters used, the “first” and “second” ones seem not to exists, and its place is taken by a very large stochastic layer. This is due to the “big” value of α required to see the fourth order meandering curve. The graphical evidence is that only for initial values of y is a very small range ($y \in (-1.347435, -1.347334)$, for $x = 0$) rotational invariant curves (i.e., not around one of the fixed or periodic elliptic points of $F_{\omega,\alpha,0}$) seem to exist. Also, in this domain some periodic islands can be seen, the ones with smaller period being 6417–periodic.

We can introduce also the notion of *period of a meander*. This is simply the period of the nearby main islands. Using the notation of (6) this corresponds to the value n. In figure 4 the periods of the first, second, third and fourth order meanders are 1, 23, 277 and

9487, respectively. In particular, last number is the period of the islands, with rotation number 411/9487, shown in d). Note that, despite first and second order meander curves do not properly exist, the related island are present.

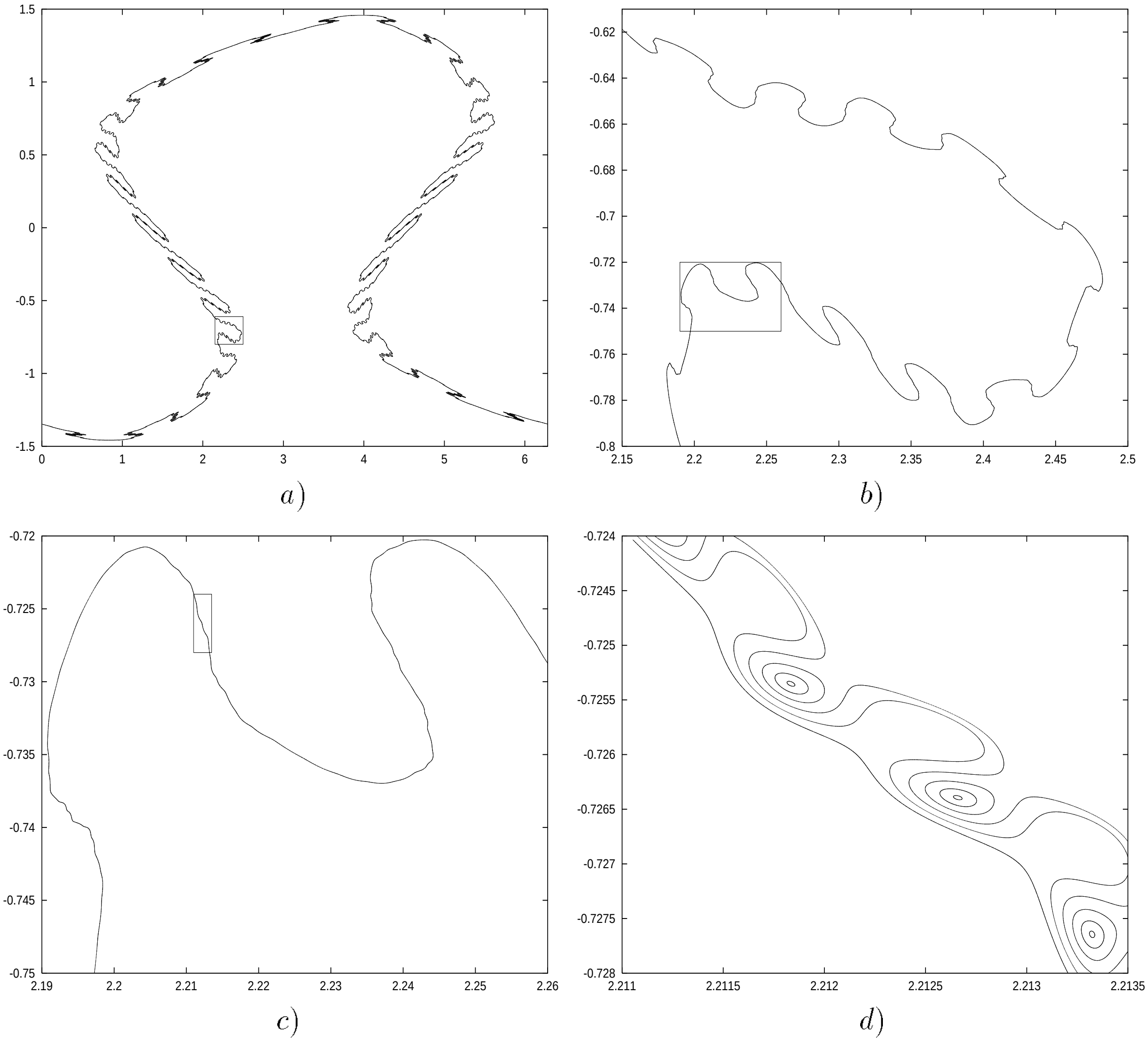

Figure 4: Higher order meandering curves. The map (18) has been used with $(\omega, \alpha, \beta) = (-0.071963192, 0.3, 0)$ and initial point $(0, -1.347394)$. The selection of (suitable ranges of) ω and y is essential here. In a) we show a global picture. Successive magnifications are shown in b), c) and d), each figure (except last one) displaying the frame of the next one. Windows: $[0, 2\pi] \times [-1.5, 1.5]$, $[2.15, 2.5] \times [-0.8, -0.61]$, $[2.19, 2.26] \times [-0.75, -0.72]$ and $[2.211, 2.2135] \times [-0.728, -0.724]$, respectively. For last picture we used also 5 additional initial values of y, with a step of 10^{-6}. In d) for each initial condition 2×10^7 iterates have been computed, only a few falling on the window. See the text for additional comments.

It is clear that, by introducing at each step suitable (and generic) small enough perturbations, one can go to any order of meandering. This seems to allow to obtain, in the limit, a nonrectifiable curve. Using the notation of (11) (see figure 1 c) for the geometrical meaning) one can introduce the *width of a meander* as the difference, along the meander, of the maximal and minimal values of y. This is related to the current value of the parameter b and can be converted to the initial variables by undoing the scalings. With the same notation, and skipping the $o(1)$ terms in (11), the *oscillation of a meander* is the difference between successive x values when a periodic orbits passes from $y=-\sqrt{b}$ to $y=\sqrt{b}$. This is a function of the current b and h: $osc= \cos^{-1}(h-2b^{3/2}/3)-\cos^{-1}(h+2b^{3/2}/3)$. To have meanders of unbounded length, one has to prove that oscillation or width do not decrease too quickly when increasing the order of the meander. It is not clear if this can be achieved inside the analytic category. Furthermore it is not clear, again, if meanders of any order can be obtained inside a generic one–parameter family of maps. The main difficulty is the accurate control of the higher order harmonics in the remainder in (17).

We return now to the case shown in figure 2 c). Using the notations introduced in Step 1, the function $p(x)$ has no harmonic with $n=2$. That is, the generic condition $c_n \neq 0$ in (9) is not satisfied. Of course, second order harmonics appear as a consequence of the interaction of the first harmonic with itself, but they are no longer the dominating ones. Concretely, let us put $\omega = 1/2+\mu/(2\pi)$ and $\beta=0$ in (18). Then $F^2_{1/2+\mu/(2\pi),\alpha,0}$ can be computed, and it turns out that the following scaling and change of variable are useful: $\mu=c\alpha^2$, $y=\alpha(z-\frac{1}{2}\sin(x))$. Denoting again the new variable z as y, the square of the map is expressed as

$$(x,y)\rightarrow(\bar{x},\bar{y})=\left(x+\alpha^2(2c+\frac{1}{4}+2y^2-\frac{1}{4}\cos(2x))+O(\alpha^4), y-\alpha^2 y\frac{1}{2}\sin(2x)+O(\alpha^4)\right),$$

which corresponds to a generating function

$$S(x\bar{y}) = x\bar{y}+\alpha^2(b\bar{y}+\frac{2}{3}\bar{y}^3-\frac{1}{4}\bar{y}\cos(2x))+O(\alpha^4), \tag{20}$$

where $b=2c+\frac{1}{4}$, and has an integrable approximation given by the time α^2 flow of the Hamiltonian

$$H(x,y)=by+\frac{2}{3}y^3-\frac{1}{4}y\cos(2x)+O(\alpha^2). \tag{21}$$

Comparing (20) with (4) we see the lack of genericity because of the absence of trigonometric terms not having $\bar{y}$ as factor, in the dominant powers of α. Note, however, that some of these terms appear inside the $O(\alpha^2)$ contribution to (20).

4 Non generic perturbations

The considerations at the end of the previous section suggest to study the effect of non-generic perturbations. One of the simplest ones has (21) as integrable approximation.

Figure 5 shows the phase portrait for different values of b. To this end some new scalings have been introduced. They amount to replace b by $-b$, $\frac{2}{3}$ by $\frac{1}{3}$ and $-\frac{1}{4}y\cos(2x)$ by $y\cos(x)$ in (21). So, we have

$$H(x,y)=-by+\frac{1}{3}y^3-y\cos(x)+O(\alpha^2). \tag{22}$$

The line $y=0$ is invariant in any case, saddle points appear at $(0,\pm\sqrt{b-1})$ if $b>1$ and centers at $(\pi,\pm\sqrt{b+1})$ if $b>-1$. For $b\in(-1,1)$ saddle points appear in $(\pm\cos^{-1}(b),0)$. At $b=1$ there is a bifurcation and the double fixed point $(0,0)$ has zero linear part, defining 6 hyperbolic sectors. The cases displayed in figure 5 correspond to $b>1$, $b=1$, $b\in(-1,1)$ and $b<-1$, respectively, from left to right.

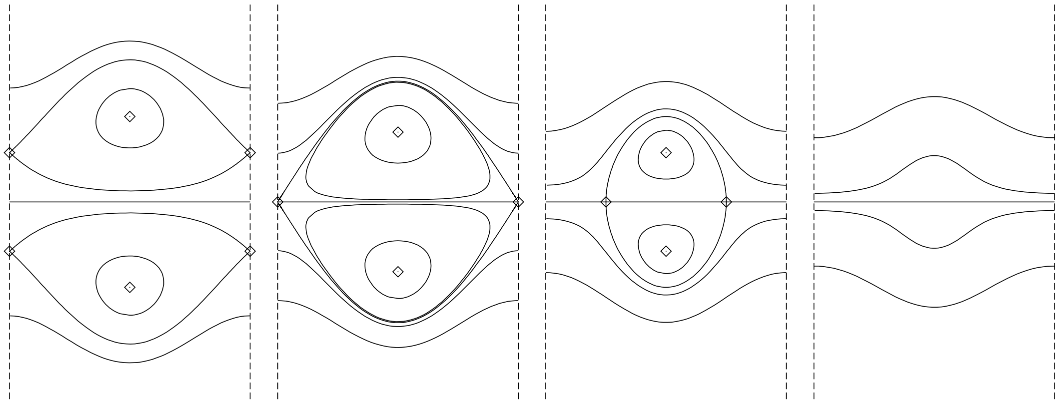

Figure 5: Several scenarios for the behavior of the Hamiltonian flow given by (21).

As it is easily seen, no meandering curves show up now in the integrable approximation. This is due to the existence of the invariant line $y = 0$. In particular, to destroy the connection between the saddles which occurs for $b \in (-1, 1)$, an additional perturbation can be introduced. The simplest thing (also guided by the previous example in figure 2 c)) consists in adding to (22) a term with a small coefficient, say d, which contains $\cos(x+\varphi)$ without any y factor. So the current Hamiltonian is

$$H(x, y) = -by + \frac{1}{3}y^3 - y\cos(x) + d\cos(x+\varphi) + o(1). \tag{23}$$

The phase φ is introduced to break symmetries. Here we think directly in terms of the Hamiltonian. The effect of this term is to move the saddles in figure 5 out of $y = 0$ and to incline, slightly, the former horizontal invariant manifolds. This produces meandering curves for the new Hamiltonian and they persist for the diffeomorphism. The full proof proceeds as for Theorem 1. It is also instructive to study the different topologies for (23) as a function of (b, d, φ).

An example is given by the family of maps

$$G_{\omega,\alpha,\beta,\varphi} : (x, y) \to (\bar{x}, \bar{y}) = \left(x + \omega + \beta\cos(x) + \bar{y}^2, \frac{y + \alpha\sin(x+\varphi)}{1 - \beta\sin(x)} \right), \tag{24}$$

where it is easy to recognize the equivalence of the parameters with the ones of the Hamiltonian: $\omega, \alpha, \beta, \varphi$ take the role of b, the normalized coefficient of $y\cos(x)$ (that is, the former α^2), d and φ, respectively.

Figure 6 a) displays an illustration, where the values of $(\omega, \alpha, \beta, \varphi)$ are taken equal to $(0, 0.01, 0.1, 1)$.

5 Higher order degeneracy of the twist

Up to now we have considered nontwist maps with the lowest possible degeneracy of the twist condition: $d\alpha/dy(y^*) = 0$, but $d^2\alpha/dy^2(y^*) \neq 0$, using the notation at §1. The study can be done in a similar way if the first nonzero derivative at y^* is the k–th one, $k > 2$. The case $k = 3$ requires, as generic perturbation, to use a Hamiltonian like

$$H_\alpha(x, y) = -by + \frac{1}{2}cy^2 + \frac{1}{4}y^4 + \cos(x) + o(1), \tag{25}$$

when the size of the perturbation goes to zero, instead of (11). As it is well known the term in y^3 can be skipped from (25) by shifting y. As one can expect, there will be, in general, 6 fixed points instead of 4, and meandering curves show up for (25). Their persistence for the APM is proved easily.

We just show here an example using the family of maps

$$C_{\omega,\alpha,\beta} : (x, y) \to (\bar{x}, \bar{y}) = (x + \omega + \beta\bar{y} + \bar{y}^3, y + \alpha \sin(x)). \tag{26}$$

The values $(\omega, \alpha, \beta) = (-0.003, 0.1, 0.4)$ have been used in figure 6 b).

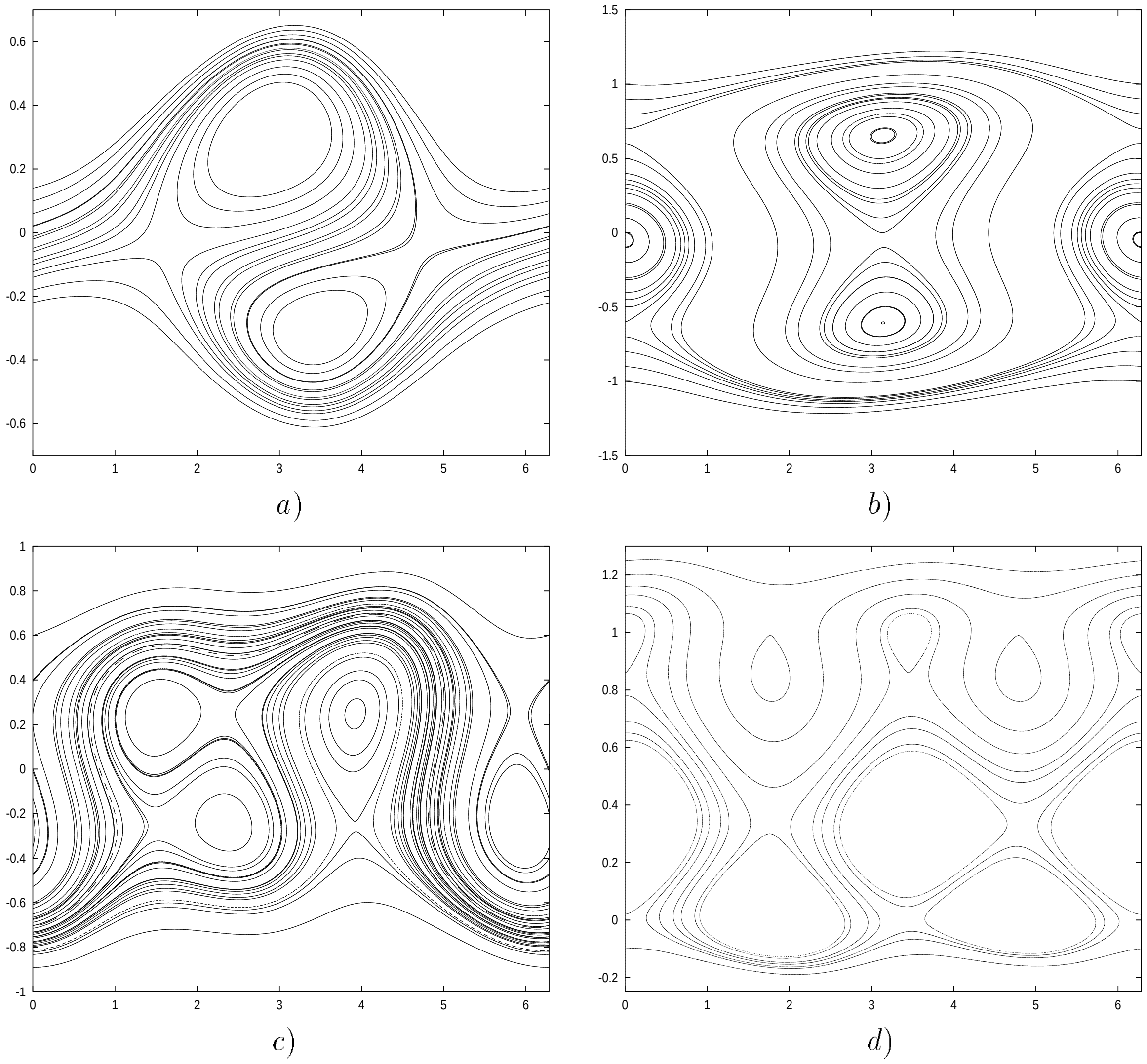

Figure 6: Several examples of meandering and labyrinthic curves. See the text for the maps and parameters used.

6 More degenerate cases. Labyrinthic curves

All the cases considered till now have a characteristic in common: Letting aside renaming the x variable, they contain, as dominant terms, only one harmonic (see (11), (21), (22) and (25)). If the nontwist is generic, but the perturbation is not, and the "second" order harmonic is as important (or more) than the "first" order one, that is, using the notation of Step 1 in the proof of Theorem 1, if c_{2n} is more important than c_n, then the suitable Hamiltonian model is

$$H_\alpha(x,y) = -by + \frac{1}{3}y^3 + \cos(x) + \frac{\gamma}{2}\cos(2x+\varphi) + o(1), \tag{27}$$

where, probably, γ can be much larger than 1. Now there appear, in general, 8 fixed points, four of them being elliptic and four being hyperbolic. A suitable selection of the values of b, γ and φ allows to obtain different patterns for the solutions of the Hamiltonian and, therefore, for the invariant curves of the APM under study.

As suggested in §4, it is instructive to study the changes of topology for (27) as a function of (b,γ,φ), to realize how the transitions due to appearence of the second hamonic take place.

We shall present a more general case and a description of the selection of parameters below. A family of maps realizing the behavior of model (27) is

$$T_{\omega,\alpha,\gamma} : (x,y) \to (\bar{x},\bar{y}) = \Big(x+\omega+\bar{y}^2, y+\alpha(\sin(x)+\gamma\sin(2x+\varphi))\Big). \tag{28}$$

An example of the possible shape of the invariant curves is shown in figure 6 c). The values of the $(\omega,\alpha,\gamma,\varphi)$ parameters used for it are $(-0.01, 0.05, 1.3, 1)$.

Looking at the shape of the different invariant curves, it seems natural to propose for them the name *labyrinthic curves*. Indeed, they look like a path on a (cylindrical) maze, the barriers of the maze being here the invariant manifolds of the saddles. These manifolds have not been displayed in figure 6 c) and d), to prevent from too many lines. Instead, some main islands have been plotted. If we look at figure 2 a) and b) we see that, following a first order meandering curve (in the (x,y) coordinates) from left to right, the tangent vector to it rotates, from a near horizontal initial angle, by some amount in $(\pi/2,\pi)$ (clockwise and counterclockwise). In figure 6 a) this rotation is close to π and in figure 6 c) it largely exceeds π. We shall see next a case where almost any angle up to 2π is admissible.

Trying to generalize the previous idea we can consider, in the simplest case, a limit Hamiltonian flow which consists of the sum of a polynomial in y (the "kinetic energy") and a trigonometric polynomial in x (the "potential"). More general situations would include products of polynomial by trigonometric functions. For concreteness we choose a polynomial of degree 5 and a trigometrical polynomial with first and second order harmonics. As we want many fixed points, we can select both of them with derivatives having 4 zeros. Scaling variables, the two extreme zeros in y can be located at $y_1 = 0$ and $y_4 = 1$. Let $0 < y_2 < y_3 < 1$ the other two. One of the zeros in x can be located at $x_1 = 0$. Let $0 < x_2 < x_3$ be two additional zeros. This fixes the fourth one, x_4. Assume x_2, x_3 are such that $x_3 < x_4$. Then, the Hamiltonian can be written as

$$H(x,y) = P(y) + \gamma T(x), \tag{29}$$

where $P'(y) = y(y-y_2)(y-y_3)(y-1)$, $\quad T'(x) = s_1\sin(x)+s_2\sin(2x)+c_1(\cos(x)-\cos(2x))$ and s_1, s_2, c_1 are choosen so that $T'(x_2) = T'(x_3) = 0$, with $s_1^2+s_2^2+c_1^2 = 1$. (Notation: $T' = dT/dx$, $P' = dP/dy$). The value of γ is a scaling factor of the potential. Hence (29) depends on 5 parameters, $p = (x_2, x_3, y_2, y_3, \gamma)$, and an APM can be derived by

$$L_{p,\varepsilon} : (x,y) \to (\bar{x},\bar{y}) = (x+\varepsilon P'(\bar{y}), y+\varepsilon T'(x)), \tag{30}$$

as usual.

The Hamiltonian H has 8 elliptic critical points and 8 saddles. Let $S_1 = (x_1, y_1)$, $S_2 = (x_1, y_3)$, $S_3 = (x_2, y_2)$, $S_4 = (x_2, y_4), \ldots$, the saddles (see figure 6 *d*)). The relative positions of the invariant manifolds depend on the values $h_j = H(S_j)$. After some tests we selected the order $h_1 < h_7 < h_5 < h_2 < h_6 < h_3 < h_8 < h_4$ as convenient for an example. Rough values of p were determined to achieve this and then they were locally optimized to maximize $\min_{i \neq j} |h_i - h_j|$, so that the "paths in the maze" allow for meandering curves of (30). The concrete values are: $x_2 = 0.2816112 \cdot 2\pi$, $x_3 = 0.549899 \cdot 2\pi$, $y_2 = 0.33040195$, $y_3 = 0.84999789$, $\gamma = -0.0049$. As in the domain of interest the vector field is small, values of ε can be taken large and still invariant curves exist. A value as large as $\varepsilon = 5$ was taken for figure 6 *d*). For values of ε between 6 and 7 some of the meanders degenerate to narrow chaotic zones.

In that figure, if we consider the main elliptic islands as holes on the cylinder, it is easy to check that the nine rotational invariant curves belong to different homotopy classes. This suggest problems like the maximal number of such nonequivalent curves as a function of the degrees of P and T.

7 Outlook

We conclude by considering some other interesting cases and open problems, that fall outside the scope of the present contribution.

- In [3] a family of APM with reversing of orientation (for short, *area reversing* or *anticonservative maps*) was introduced. It is a limit, conservative, case of a 3–parameter family of maps (denoted in [3] as *fattened Arnol'd map*) describing a kind of "universal" and "global" model for near homoclinic tangencies of dissipative diffeomorphisms. It is given by

$$ASM_{\omega,\alpha}(x, y) = (x + \omega + y + \alpha \sin(x), -(y + \alpha \sin(x)). \tag{31}$$

It can be considered as a map on $\mathbb{T}^2$. This expression suggests to name it *anti–standard map*. In contrast with the standard map, the parameter ω can not be skipped by a shift of variables. The change of variables $(\xi, \eta) = (x, x + y + \omega)$ reduces it to

$$AC_{\omega,\alpha}(\xi, \eta) = (\eta + \alpha \sin(\xi), \xi + 2\omega). \tag{32}$$

The symmetry $(\xi, \eta, \alpha, \omega) \leftrightarrow (-\xi, -\eta, \alpha, -\omega)$ and how ω appears in (32) show that it is enough to consider $\omega \in [0, \pi/2]$. Several dynamical properties, the occurrence of meandering curves on (31) and the relation to several other maps are presented in [3].

Going back to (31) the square is given by

$$ASM^2 \begin{pmatrix} x \\ y \end{pmatrix} = \begin{pmatrix} x + 2\omega + \alpha \sin(x + \omega + y + \alpha \sin(x)) \\ y + \alpha \sin(x) - \alpha \sin(x + \omega + y + \alpha \sin(x)) \end{pmatrix}. \tag{33}$$

This is an APM, but it is far from "general". Indeed, for $\alpha = 0$ there is no twist at all ($d\alpha/dy \equiv 0$). The oscillating character of the term which contains y in $\bar{x}$ prevents even from a "weak" twist property of order α. Anyway, if ω is not a multiple of $\pi/2$, there is a range of α around 0 for which invariant curves exist. The reason of that behavior is that the map has a "very weak" twist condition but an even weaker perturbation. This result is be obtained by a suitable averaging.

It would be interesting to study, in general, this kind of "extra" degeneration, i.e., the cases in which the twist condition (if any) can be recovered by averaging an oscillating function along the dynamics.

- An extremely interesting problem appears when higher dimensional symplectomorphisms are studied. A small perturbation of the product of one of the nontwist maps considered here and a twist map, can give nice invariant tori. Coupling two nontwist maps should produce some amazing "higher dimensional labyrinths". But now there are extra dimensions to escape from the maze.

  The simplest case appears when the vicinity of a totally elliptic point, near a double resonance, is analyzed. Some simple conditions allow to have degenerate torsion. Work in that direction is in progress.

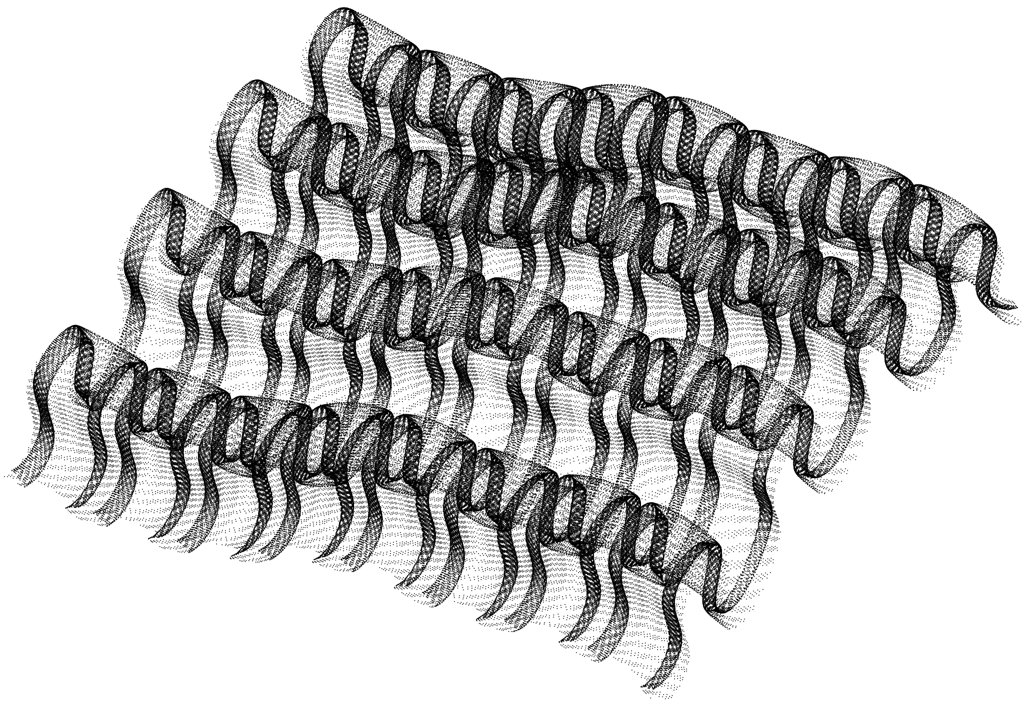

Figure 7: A 3D view of a meandering 2D torus of the map (34) for the parameters given in the text. The 2D torus is projected on the variables $x_1, x_2, y_1 + y_2$ before displaying the 3D view.

Figure 7 shows an illustration of a "meandering torus" for a symplectic map in dimension four. It is a 2D torus. The map used to generate it is

$$F\begin{pmatrix} x_1 \\ x_2 \\ y_1 \\ y_2 \end{pmatrix} = \begin{pmatrix} \bar{x}_1 \\ \bar{x}_2 \\ \bar{y}_1 \\ \bar{y}_2 \end{pmatrix} = \begin{pmatrix} x_1 + 2\pi\omega_1 + \bar{y}_1^2 + \psi\bar{y}_1\bar{y}_2 \\ x_2 + 2\pi\omega_2 + \bar{y}_2^2 + 0.5\psi\bar{y}_1^2 \\ y_1 + \alpha_1 \dfrac{\sin(x_1)}{1-\beta_1\cos(x_1)} \\ y_2 + \alpha_2 \dfrac{\sin(x_2)}{1-\beta_2\cos(x_2)} \end{pmatrix}, \tag{34}$$

that is, the coupling of two maps like the $F_{\omega,\alpha,\beta}$ given in (18). The current parameters have been choosen to be the ones used in figures 2 a) and b), that is $\omega_1 = 0.249$, $\alpha_1 = 0.1$, $\beta_1 = 0.5$, $\omega_2 = 0.374675$, $\alpha_2 = 0.1$, $\beta_2 = 0.5$, while the coupling ψ has been taken equal to 0.03. As initial conditions $x_1 = x_2 = 0$, $y_1 = -0.039$, $y_2 = -0.202$ have been selected, and 500,000 iterates are done. The figure shows a 3D view of the projection of the invariant meandering 2D torus on the space of the variables $x_1, x_2, y_1 + y_2$. We want to remark that, for values of ψ slightly larger, all 2D tori seem to be destroyed.

Acknowledgements

This work was supported by the DGICYT PB94–0215 grant (Spain) and the CIRIT 1996S0GR-00105 grant (Catalonia). Partial support of the European Network Grant ERBCHRXCT 940460 and INTAS grant 93-0339ext is also acknowledged. A first version of these results was presented at a Workshop on Dynamical Systems at the Universitat Autònoma de Barcelona in September 97. I am indebted to the organizers of that event.

References

[1] Arnol'd, V. I.: Proof of A. N. Kolmogorov's theorem on the preservation of quasi–periodic motions under small perturbations ofi the Hamiltonian, *Usp. Mat. Nauk SSSR* **18** no. 5 (1963), 13–40.

[2] Broer, H., Roussarie, R., Simó, C.: Invariant circles in the Bogdanov-Takens bifurcation for diffeomorphisms. *Ergod. Th. & Dynam. Sys.*, **16** (1996), 1147-1172.

[3] Broer, H., Simó, C., Tatjer, J. C.: Towards global models near homoclinic tangencies of dissipative diffeomorphisms, *Nonlinearity*, **11**(3) (1998), 667–770.

[4] Haro, A.: *The Primitive Function of an Exact Symplectomorphism*, Ph. D. Thesis, Universitat de Barcelona, 1998.

[5] Herman, M.: Sur les courbes invariantes par les difféomorphismes de l'anneau, *Astérisque*, **103–104**, 1983.

[6] Herman, M.: Dynamics connected with indefinite normal torsion, in *Twist Mappings and Their Applications*, Ed. R. M. McGehee and K. R. Meyer, IMA Vol. **44**, Springer–Verlag, 1992.

[7] Kolmogorov, A. N.: Théorie générale des systèmes dynamiques et mécanique classique, *Proc. Int. Congress of Math., Amsterdam*, 1957. Translation in Appendix D of Abraham, R., *Foundations of Mechanics*, Benjamin, 1967.

[8] Moser, J.: On invariant curves of area–preserving mappings of an annulus, *Nachr. Akad. Wiss., Göttingen, Math. Phys. Kl.* (1962), 1–20.

[9] Neishtadt, A. I.: The separation of motions in systems with rapidly rorating phase, *Prikladnaja Matematika i Mekhanika* **48** (1984), 133–139.

[10] Nikitin, A.: Separatrix splitting for the 'twist map'. A method of calculation of the coefficients of the splitting formula. *Math. Preprint Series* **184** (1995), Universitat de Barcelona.

[11] Rüssmann, H.: Über invariante Kurven differenzierbarer Abbildungen eines Kreisringes, *Nachr. Akad. Wiss., Göttingen II, Math. Phys. Kl.* (1970), 67–105.

[12] Siegel, C. L., Moser, J. K.: *Lectures on Celestial Mechanics*, Grundlehren Bd. **187**, Springer–Verlag, 1971.

[13] Simó, C., Treschev, D.: Stability islands in the vicinity of separatrices of near–integrable symplectic maps. Preprint, 1997.

[14] Simó, C., Treschev, D.: Evolution of the "last" invariant curve in a family of area preserving maps: The case of the separatrix map, preprint, 1997.

[15] Zaslavsky, G., Zakharov, M., Sagdeev, R., Usikov, D., Chernikov, A.: Stochastic web and diffusion of particles in a magnetic field, *Zh. Eksp. Teor. Fiz.*, **91** (1986) 500–515.